# The nucleotide-free state of heterotrimeric G proteins α-subunit adopts a highly stable conformation

Sai Krishna Andhirka, Ravichandran Vignesh and Gopala Krishna Aradhyam

Department of Biotechnology, Bhupat and Jyoti Mehta School of Biosciences, Indian Institute of Technology Madras, Chennai, Tamil Nadu, India

Deciphering the mechanism of activation of heterotrimeric G proteins by their cognate receptors continues to be an intriguing area of research. The recently solved crystal structure of the ternary complex captured the receptor-bound α-subunit in an open conformation, without bound nucleotide has improved our understanding of the activation process. Despite these advancements, the mechanism by which the receptor causes GDP release from the α-subunit remains elusive. To elucidate the mechanism of activation, we studied guanine nucleotide-induced structural stability of the α-subunit (in response to thermal/chaotrope-mediated stress). Inherent stabilities of the inactive (GDP-bound) and active (GTP-bound) forms contribute antagonistically to the difference in conformational stability whereas the GDP-bound protein is able to switch to a stable intermediate state, GTP-bound protein loses this ability. Partial perturbation of the protein fold reveals the underlying influence of the bound nucleotide providing an insight into the mechanism of activation. An extra stable, pretransition intermediate, 'empty pocket' state (conformationally active-state like) in the unfolding pathway of GDP-bound protein mimics a gating system – the activation process having to overcome this stable intermediate state. We demonstrate that a relatively more complex conformational fold of the GDP-bound protein is at the core of the gating system. We report capturing this threshold, 'metastable empty pocket' conformation (the gate) of α-subunit of G protein and hypothesize that the receptor activates the G protein by enabling it to achieve this structure through mild structural perturbation.

## Introduction

G proteins act as important molecular switches, cycling between OFF (GDP-bound) and ON (GTP-bound) states, regulating the strength and duration of the cellular response to a signal detected by its cognate G protein-coupled receptor (GPCR) [1–3]. Since the elucidation of the recent crystal structure of GPCR: G protein ternary complex, the α-subunit of G proteins has regained central focus in signal transduction [4]. The structure of the α-subunit in the complex was a surprise due to two novel features: (a) large structural movement of the helical domain (HD) and (b) the protein crystallizing without the nucleotide. The structure of the ternary complex reinforces earlier proposed models of GDP release: (a) opening of the interdomain cleft and (b) involvement of α5 helix in releasing the nucleotide [5–12].

Whereas both N- and C-terminal regions of the α-subunit are important in binding to the activated

receptor, other regions (e.g., α3- α5 and α4- α6 loops and parts of the HD) are crucial for completing the GTPase cycle, by interacting with the downstream effectors. Charge diversity observed in these regions, among various types of α-subunits, leads to differences in downstream associating partners and signaling pathways also influencing activation/deactivation rates [6]. Electron microscopy studies of the receptor: G protein ternary complex demonstrate the conformational flexibility and highly variant positions of the HD (with respect to Ras-like domain) in the α-subunit upon loss of the bound nucleotide, providing a clue to diverse structural changes in the process of activation [13]. However, whether the large movement of the domains is the cause or the consequence of nucleotide release is still unclear and crystal structure could be one among an ensemble of structures that the protein searches in order to attain a stable conformation. As signaling involves interactions among multiple proteins, the interface of the α-subunit and its interacting partners, and its interdomain interactions are of central importance, a structural consequence of its design principle [1,3,6].

There are scarce reports that relate activation mechanism of G proteins with their structural complexity [14–16]. Even as the structural changes between the inactive and active state of the protein are known, only a single study of heterotrimeric G proteins reports increased the rate of GTP uptake by a G202D mutant in Gα$_{i1}$, attributed to the protein's attenuated conformational/structural stability [14]. That the differential intricacies of the structural fold of the protein are driven by the underlying influence of bound nucleotide has not been explored. On the basis of investigations reported here, we argue that the solution state structural stabilities of G proteins can be used as a probe to study the mechanism of its activation. Differential structural complexity and stability of Gα$_{i1}$ (GDP-bound compared to the GTP-bound) steered us to demonstrate that partial structural perturbation of Gα$_{i1}$.GDP (by guanidinium chloride, GdmCl) results in a 'metastable intermediate state' without a bound nucleotide. Support for the proposed mechanism is also gained by (a) studying select Gα$_{i1}$ mutants and (b) using cytoplasmic loop peptides of the OA1 receptor (a relatively new, melanosomal GPCR) [17]. Our results demonstrate the trapping of an empty pocket and stable state structure of Gα upon mild structural perturbation. We propose that activated GPCRs aid in achieving this structural state of the Gα as a first step in the process of activation. Our observations offer an avenue to study the detailed conformational fold of the 'empty pocket' state of the α-subunit (Fig. 9).

# Results

## The structural complexity of the 'off-state' G protein is lost upon activation

The influence of bound nucleotide on the thermodynamic stability and the relative unfolding complexity (multiple structural intermediates as observed, exclusive of each other) of the structure of Gα$_{i1}$ and its relationship with the mechanism of activation were investigated by thermal perturbation of its structure. Stability of Gα$_{i1}$ in GTP-bound conformation [apparent transition temperature ($T_m$) is 70 °C] is significantly higher than the AlF$_4^-$- ($T_m$ = 55 °C) or GDP-bound ($T_m$ = 50 °C) conformations, with a highly cooperative unfolding transition pattern (evident from the characteristic sigmoidal shape of the thermograph; Fig. 1). That the difference in stability is specifically achieved for the function is evident from the preliminary work of Johnston *et al.* [14] – a G202D mutation causing a loss in structural stability of the protein and thereby affecting its function. In this work, we demonstrate that it is the complexity of the G protein's fold that differentiates the '(GTP-bound) on' state from the
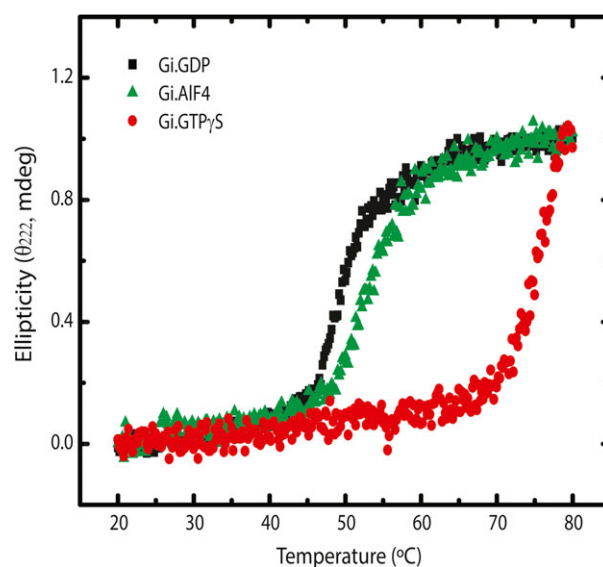


**Fig. 1.** Thermal unfolding of Gα$_{i1}$ reveals differential conformational stabilities for the inactive and activated states. The structural stability of Gα$_{i1}$ was monitored using CD spectroscopy. Ellipticity values at 222 nm are plotted against temperature. AlF$_4^-$ binding produces a transition state analog in the activation pathway. The nucleotide exchange in GDP for GTP in Gα$_{i1}$ was initiated by incubation with 100 μM GTPγS (50-fold excess), on ice for 1 h. $T_m$ is highest for GTP-bound protein (red trace, 77 °C) followed by AlF$_4^-$-bound (green trace 55 °C) and GDP-bound protein (black trace 50 °C).

'off' state. We demonstrate that the 'GDP-bound off-state' structure has the capacity to adopt a highly stable nucleotide-free intermediate fold that mimics the 'GTP-bound active state' (in its stability profile). To understand the mechanism of G protein activation by the receptor, we use the stability status of the protein as a readout and establish that the design principle of GDP-bound G protein enables it to adopt a highly stable 'empty pocket' conformation, which leads to activation–GTP uptake.

Toward elucidating this goal, we perturbed the structure of different forms of $G\alpha_{i1}$ (GDP-bound, $AlF_4^-$-bound and GTP-bound). Chemical perturbations (underequilibrium conditions) reveal a complex open-to-close transition of the $G\alpha_{i1}$ in the GDP-bound state but not in the GTP-bound form, providing an insight into the mechanism of activation. The GDP-bound form experiences an ~ 8 nm blue shift of fluorescence emission maxima at submolar concentration of GdmCl (tryptophan residues reporting a more compact structure), accompanied by a sharp decrease in fluorescence and circular dichroism (CD) signal, followed by a red shift and resurgence of fluorescence signal followed by an increase in ellipticity of CD signal between 0.8 and 1.5 M GdmCl (Fig. 2A and D). This indicates the propensity of GDP-bound $\alpha$-subunit to remodel its global structure and attain a more compact fold (Inset of Fig. 2A). A similar process was not observed in GTP-bound form, where a loss of structure begins well above 1 M GdmCl (Fig. 2C and F). In contrast with GDP- or GTP-bound states, the $AlF_4^-$-bound state of $G\alpha_{i1}$ represents the intermediate structural complexity of unfolding transitions (Fig. 2B and E). The final transition to completely unfolded state in all cases begins at 4 M GdmCl, evident by a shift of the fluorescence emission maxima toward higher wavelengths
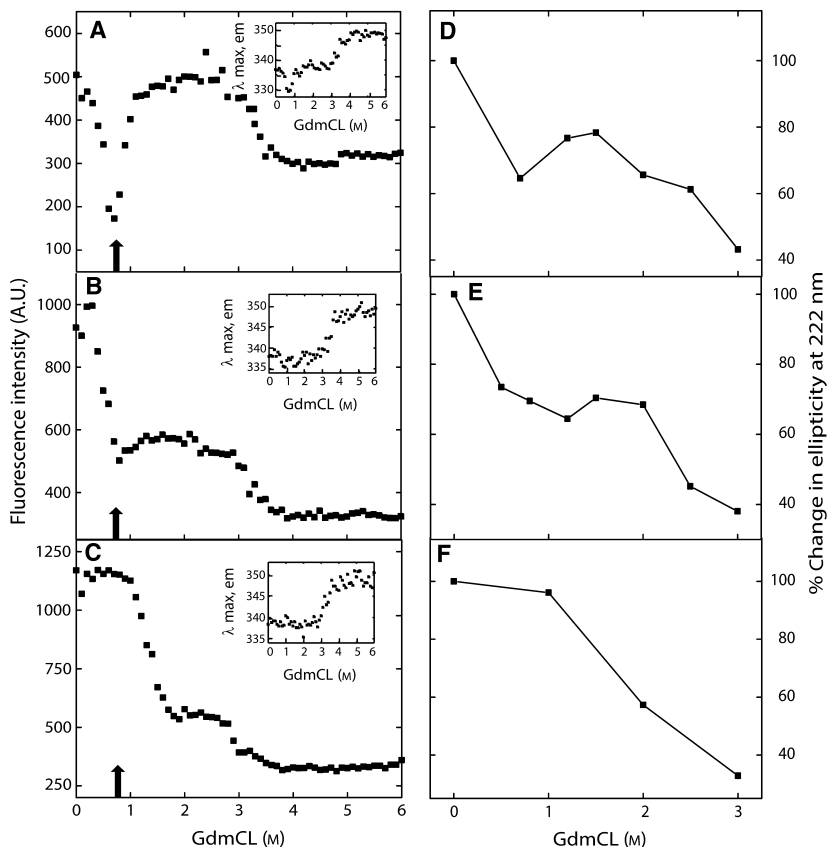


**Fig. 2.** Unfolding path of $G\alpha_{i1}$ reveals nucleotide-dependent multiple conformational states. Conformational changes in $G\alpha_{i1,}$ observed in different nucleotide-bound states, due to the effect of GdmCl (0–6 M) were monitored by intrinsic tryptophan fluorescence and CD spectroscopy. Panels A, B, and C represent the fluorescence intensity at 340 nm of GDP-bound, $AlF_4^-$- and GTPγS-bound $G\alpha_{i1}$ (55 μg·mL$^{-1}$), respectively, as a function of GdmCl concentrations. The inset in each of these panels is the plot of wavelength maxima ($\lambda_{max}$) as a function of GdmCl concentration. Arrow indicates the fluorescence data point at 0.7 M GdmCl. Panels D, E, and F represent the percent change in ellipticity at 222 nm of GDP-bound, $AlF_4^-$- and GTPγS-bound $G\alpha_{i1}$ (5.5 μM), respectively, as a function of GdmCl concentrations. The ellipticity value at 0 M GdmCl was considered to be 100% and relative change in the signal is depicted as percent values.

(red shift confirming unfolded protein; Insets of Fig. 2A,B,C).

## Activation proceeds through a metastable intermediate state

The activation process of G proteins is achieved by the receptor-mediated release of the bound GDP from the α-subunit and consequent uptake of GTP. The complex structural features adopted by the α-subunit (demonstrated in its unfolding path) and the fact that GDP release is the rate-limiting step prompted us to hypothesize that the α-subunit experiences an additional stable structure in the GTPase cycle. Upon perturbations by GdmCl and monitoring the fluorescence changes, the thermodynamic parameters for the unfolding of $G\alpha_{i1}$ in GDP-, $AlF_4^-$-, GTP-bound form were calculated as mentioned in methods (Table 1), indicating the conformational stability of $G\alpha_{i1}$ in various ligand-bound forms. The fractions of native, intermediate, and unfolded states (calculated from the fluorescence data) when plotted as a function of GdmCl concentration indicate their distribution in the unfolding transitions. GDP-bound conformation follows a path with two intermediate states whereas $AlF_4^-$ and GTP-bound conformation follows a path with a single intermediate (Fig. 3). This reinforces our activation model that the α-subunit is capable of adopting two different structural conformations including a very stable nucleotide-free conformation [the function of the receptor being to push the protein to attain the stable 'empty pocket transition state' (metastable state that can be trapped – see later)], enabling nucleotide release and holding the protein in an activatable form.

Structural stability of wild-type (WT) $G\alpha_{i1}$ and its mutants were assessed by thermal stabilities of the

protein employing the techniques of fluorescence, CD spectroscopy, and differential scanning calorimetry (DSC; Table 2). We demonstrate that one of the stepwise variant conformations in the activation process, a structurally compact form (in the GTPase-cycle with GDP-$G\alpha_{i1}$), is held as a metastable intermediate and that it can be trapped at about 1 M GdmCl. The difference in $T_m$ (as mentioned earlier) among the various ligand-bound states in the GTPase cycle is exploited here to monitor the complex conformational state of the protein at ∼ 1 M GdmCl. We demonstrate that this minor perturbation of the global conformation of the (GDP-bound) protein leads to protein's $T_m$ escalating close to 70 °C, thereby mimicking the (GTP-bound) active state conformation and hence enabling an opportunity to trap this novel metastable intermediate state (Fig. 4A,B). The new compact structure so attained (around 1 M GdmCl) provided a lead and prompted us to examine for any liaison between the stability of this intermediary state and the mechanism of activation. It is also possible that the conditions reported here may be replicating (structurally) those created by 'Ric' proteins, known to stabilize the empty pocket state [18].

## Trapping the metastable intermediate and the structure of empty pocket Gαi1

The activity of G proteins is also routinely assessed by the binding of $AlF_4^-$ or GTP analogues, monitoring a conformational switch leading to an increase in fluorescence emission from a tryptophan residue (at position 211, W211) in the switch II region of the protein (due to its movement into a nonpolar environment) [19–21]. Here, we illustrate trapping 'empty pocket' state of the protein and demonstrate its propensity for

**Table 1.** Thermodynamic parameters for the GdmCl-induced unfolding of Gαi1 in GDP, $AlF_4^-$ and GTPγS bound conformations monitored by fluorescence. The unfolding transitions were fitted to the equations (as described under Materials and methods section) by least-square analysis using GRAPHPAD Prism version 5.0. The standard error (SE) values are indicated. The unit for $\Delta G°$ is kcal·mol$^{-1}$, and the unit for 'm' is kcal·mol$^{-1}$·M$^{-1}$.

|  | GDP bound Gαi1 | $AlF_4^-$ bound Gαi1 | GTPγS bound Gαi1 |
|---|---|---|---|
| $\Delta G°_1$ (kcal·mol$^{-1}$) | 3.8 ± 0.8 | 4.2 ± 0.8 | 6.0 ± 0.4 |
| $m_1$ (kcal·mol$^{-1}$·M$^{-1}$) | 6.7 ± 2.1 | 8.5 ± 1.5 | 4.5 ± 0.3 |
| $D_{50\%}$ (M) | 0.48 | 0.5 | 1.33 |
| $\Delta G°_1$ (kcal·mol$^{-1}$) | 4.1 ± 1.5 | 8.7 ± 1.4 | 9.8 ± 1.7 |
| $m_1$ (kcal·mol$^{-1}$·M$^{-1}$) | 5.0 ± 1.3 | 2.8 ± 1.3 | 3.3 ± 0.6 |
| $D_{50\%}$ (M) | 0.93 | 3.1 | 2.94 |
| $\Delta G°_1$(kcal·mol$^{-1}$) | 13.6 ± 2.5 | – | – |
| $m_1$ (kcal·mol$^{-1}$·M$^{-1}$) | 4.2 ± 0.8 | – | – |
| $D_{50\%}$ (M) | 3.2 | – | – |
| Global $\Delta G°_{N-D}$ (kcal·mol$^{-1}$) | 21.5 ± 4.8 | 12.9 ± 2.2 | 15.8 ± 2.1 |
| Global $m$ (kcal·mol$^{-1}$·M$^{-1}$) | 15.9 ± 4.2 | 11.3 ± 2.0 | 7.8 ± 0.9 |
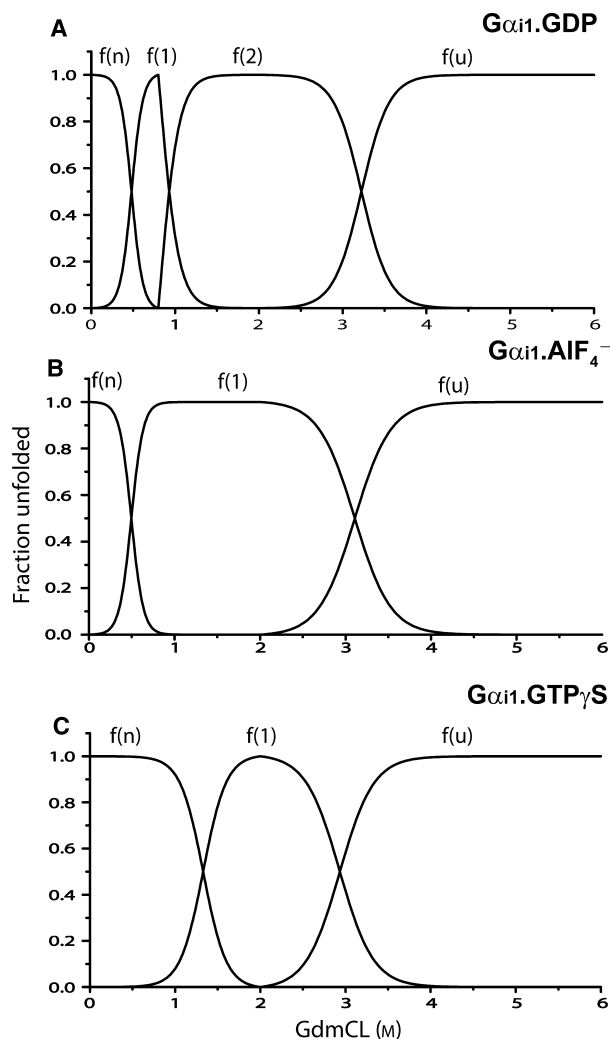
**Fig. 3.** Gα$_{i1}$ in GDP-bound form exhibits an intermediate state in its unfolding path. The fractions of the native (fn), first intermediate (f1), second intermediate (f2), and unfolded (fu) states were calculated using parameters deduced from the fits of the unfolding transitions. The values of parameters $\Delta G°_1$, $\Delta G°_2$, $\Delta G°_3$, $m_1$, $m_2$, and $m_3$ for GDP-bound Gα$_{i1}$ were determined using the nonlinear least square fitting (GRAPHPAD Prism) to the unfolding data using the four state equation. $\Delta G°_1$, $\Delta G°_2$, and $\Delta G°_3$ represent the free energy change in each step and $m_1$, $m_2$, and $m_3$ represent the free energy dependence on denaturant concentration [D] associated with each step. The values of YN, Y1, Y2, and YU representing signal from each species estimated graphically (set as constant during the fit) and the corresponding GdmCl concentrations were used as a reference point to represent the fractional populations. Each fractional transition step depicted graphically is calculated and fit from residuals of a two-state equation. Similarly, the parameters were calculated for three state model of AlF$_4^-$ and GTPαS-bound Gα$_{i1}$, respectively, and fractional populations were depicted as described above. (A) Gα$_{i1}$ in GDP-bound state; (B) Gα$_{i1}$ in AlF$_4^-$-bound state; (C) Gα$_{i1}$ in GTPγS-bound state.

activation by uptake of GTP but not by AlF$_4^-$ binding (due to lack of bound GDP). Rates of GTPγS uptake initially decreased at 0.1 M GdmCl but markedly increased between 0.1 and 0.7 M GdmCl accompanied by a decrease in 'saturation plateaus' (Fig. 4C). At 0.7 M GdmCl, the protein exhibits rapid uptake of GTPγS but does not get activated by AlF$_4^-$, implying that partial unfolding or perturbance of the structure causes the release of the bound GDP, trapping the 'empty pocket state' (Fig. 5B). The protein loses its conformational fidelity for nucleotide exchange at 0.7 M GdmCl, a state of minimum secondary structure (Fig. 2A and D). Further incremental unfolding leads to drastic global conformational changes accompanied by enhancement of the secondary structure (Fig. 2D) and meta-stabilization of the empty pocket structure at 1 M GdmCl (Fig. 4A). It is noteworthy that previous attempts of trapping the similar conformational state of the protein led to its aggregation [22,23], whereas in our case, the presence of GdmCl probably stabilizes it against aggregation.

## Empty pocket state can also be trapped during refolding

The alpha subunit of G proteins undergo the GDP/GTP cycle and hence it is important to demonstrate the ability of the protein to attain the empty pocket state in the process of refolding. Reversibility of the structural changes caused by the controlled removal of GdmCl is demonstrated by observing the patterns of activity and dynamics in the refolding process of Gα$_{i1}$. As seen in Fig. 5A, the secondary structure of the refolded protein is in close resemblance to that of the native protein. Concurrently, the biological activity (monitored by nucleotide exchange) and elevated thermal stability at 1 M GdmCl was also restored in the refolded protein (Fig. 6A). A closer look at our results reveal that, though the unfolding and refolding paths followed by the protein are overlapping (Fig. 5A), there are marked differences in certain instances when the thermal stabilities of the protein are studied in similar conditions (unfolded to 0.5 M or refolded to 0.5 M). As in the case of WT (unfolded by 1 M GdmCl), the refolded protein also demonstrates an increase in $T_m$ from ~ 55 to ~ 72 °C at 1 M GdmCl. The differences in the stabilities depicted at 0.5 M GdmCl could be a consequence of multivaried interactions in the protein and the Guanidine group of GdmCl [24,25]. From these data, it is evident that in the process of refolding GDP binds back to the

**Table 2.** Comparison of $T_m$ from fluorescence, CD and DSC. The structural stabilities (apparent $T_m$) of WT Gαi1 and its point mutants in their GDP and GTPγS bound states derived from fluorescence, CD and DSC data are listed. The bold faced values correspond to apparent $T_m$ of GDP bound Gαi1–ICL3 peptide complex. However, the spectra for Gαi1–ICL3 peptide complex from fluorescence and DSC could not be obtained due to scattering and aggregation effects of the complex respectively. The comparison of wild-type and mutants apparent $T_m$'s clearly illustrates the selective destabilizing effect on the GDP bound conformation by ICL3 peptide but not on their GTP bound state.

| | | Melting temperature ($T_m$) °C | | | | | |
| | | Fluorescence | | CD | | DSC | |
| Protein | Peptide | GDP bound | GTPγS bound | GDP bound | GTPγS bound | GDP bound | GTPγS bound |
|---|---|---|---|---|---|---|---|
| WT Gα$_{i1}$ | No peptide | 52.5 | 72 | 50 | 75 | 49.5 | 72.5 |
| | ICL1 | 47.5 | 72 | 50 | 75 | 49.5 | 72.2 |
| | ICL3 | – | – | **46** | 75 | – | – |
| | ICL4[F] | 47.5 | 72 | 50 | 75 | 49.5 | 72.5 |
| Gα$_{i1}$ G203A mutant | No peptide | 57.5 | 57.5 | 47.5 | 62.5 | 47.2 | 52.5 |
| | ICL1 | 57.5 | 57.5 | 47.5 | 62.5 | 47.2 | 55.5 |
| | ICL3 | – | – | **45** | 62.5 | – | – |
| | ICL4[F] | 57.5 | 57.5 | 47.5 | 62.5 | 47.2 | 54.5 |
| Gα$_{i1}$ Q204L mutant | No peptide | 59 | 67.5 | 50 | 70 | 49.2 | 71.2 |
| | ICL1 | 55 | 67.5 | 5 | 70 | 49.2 | 71.2 |
| | ICL3 | – | – | 47.5 | 70 | – | – |
| | ICL4[F] | 55 | 67.5 | 50 | 70 | 49.2 | 71.2 |
| Gα$_{i1}$ A326S mutant | No peptide | 55 | 64 | 52.5 | 65 | 43.5 | 67.5 |
| | ICL1 | 55 | 62.5 | 52.5 | 65 | 43.5 | 72.5 |
| | ICL3 | – | – | 42.5 | 65 | – | – |
| | ICL4[F] | 55 | 60.5 | 52.5 | 65 | 42.5 | 69.2 |
| Gα$_{i1}$ T329A mutant | No peptide | 55 | 60.5 | 49 | 67.5 | 42.5 | 65 |
| | ICL1 | 50 | 60.5 | 49 | 67.5 | 42.5 | 69.2 |
| | ICL3 | – | – | 42 | 67.5 | – | – |
| | ICL4[F] | 49 | 60.5 | 49 | 67.5 | 42.5 | 67.5 |

protein and even enables its activation. Supporting our observation regarding the existence of the 'empty pocket' state of the protein above 0.5 M GdmCl, Gα$_{i1}$ loses its ability to be activated by AlF$_4^-$ because of the lack of bound GDP (nucleotide-free state) in a concentration (of GdmCl) dependent manner. On the other hand, a concurrent rapid uptake of GTPγS is noticed implicating that the protein structure is intact for activation (Fig. 5B). Furthermore, the increase in activity (compared to unfolded protein) for the refolded protein at certain concentrations of GdmCl is probably because of the interaction of the guanidine groups of GdmCl with the core of the protein, where arginine side chains were supposed to have been present [26]. This possibly leads to a structural stabilization that enables a faster uptake and better fit (binding) of the GTP, leading to an increase in activity (Fig. 5B). The structural stability of refolded Gα$_{i1}$ is further demonstrated by analyzing the tertiary structural changes using near-UV CD spectroscopy of unfolded and refolded protein revealed an improvised tertiary structure (Fig. 6B).

## The receptor selectively drives only the GDP-bound conformation of Gα to a metastable state

The mechanism by which GPCRs activate G proteins was investigated by studying the effect of intracellular peptides of OA1 receptor on the basal nucleotide exchange rates and thermal stabilities of Gα$_{i1}$ and its mutants. Four well-studied mutants of Gα were also selected based on the differences in their conformational statuses and rates of activation. The mutations A326S and T329A, located in the α5 helix region (proximal to the C-terminus), lead to higher basal GDP release rates resulting in faster nucleotide exchange [7,27,28]. In contrast, G203A and Q204L mutations, located in the switch-II region, exhibit altered activities without any effect on the basal GDP release rates (Fig. 7G, Table 3). The replacement of glutamine by leucine in Q204L mutant abolishes the intrinsic GTPase activity and renders it constitutively active [29]. On the other hand, G203A mutant has reduced Mg$^{2+}$ affinity and is unable to dissociate from βγ dimer upon GTP binding rendering it completely inactive [30]. In this study, the measured rates
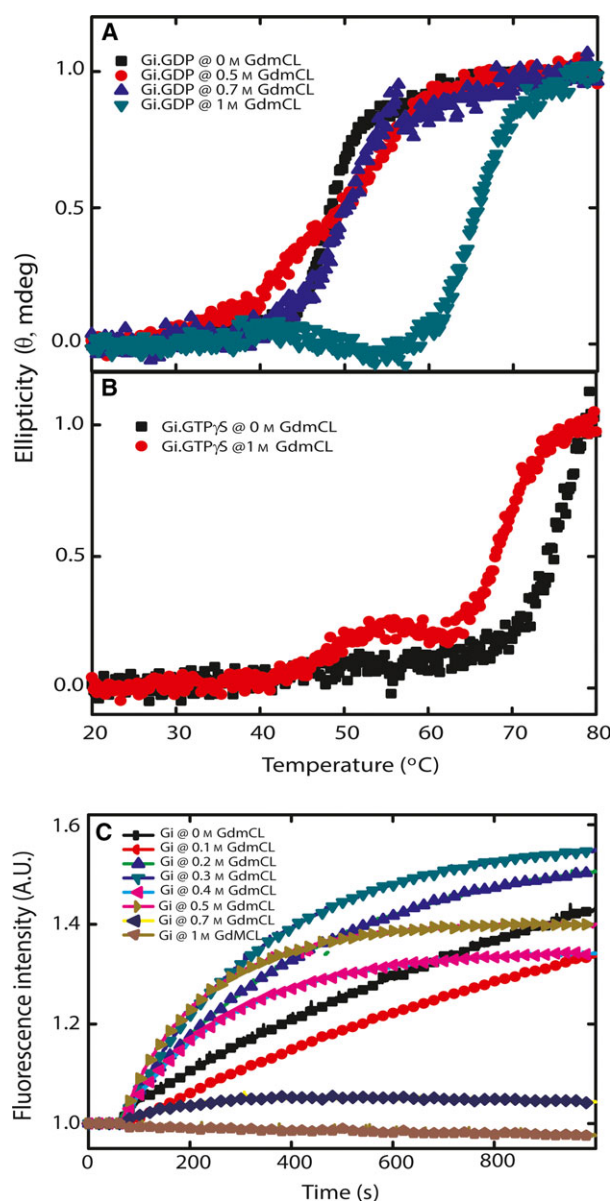
**Fig. 4.** The 'metastable intermediate state' of $G\alpha_{i1}$ is activatable. The ellipticity value at 222 nm (representative of the secondary structure content) was plotted as a function of temperature to monitor the global unfolding of $G\alpha_{i1}$ (5.5 μM). Panel A represents $G\alpha_{i1}$.GDP in 0 M (black trace, apparent $T_m$ is 50 °C), 0.5 M (red trace, apparent $T_m$ is 50 °C), 0.7 M (blue trace, apparent $T_m$ is 50 °C) and 1 M (dark cyan trace, apparent $T_m$ is 65 °C) GdmCl. Similarly, Panel B represents $G\alpha_{i1}$. GTPγS in 0 M (black trace, apparent $T_m$ is 77 °C) and 1 M GdmCl (red trace, apparent $T_m$ is 77 °C). Experiments were performed in HEPES buffer. The fluorescence emission of 200 nM protein at 340 nm ($\lambda_{ex}$ = 295 nm) was plotted as a function of time to monitor the activation kinetics in different concentrations of GdmCl. Panel C depicts the activation time course of $G\alpha_{i1}$ (after the addition of 50 μM GTPγS) in 0 M (black), 0.1 M (red), 0.2 M (blue), 0.3 M (dark cyan), 0.4 M (magenta), 0.5 M (dark yellow), 0.7 M (navy), and 1 M (brown) GdmCl.

of activation of these mutants are consistent with previous reports, including their activation traces following the tryptophan fluorescence (Fig. 7G) [7,27]. We have used these mutants of the α-subunit as a representative ensemble of conformational folds (as probable steps in the mechanism of activation) in our quest to better understand the mechanism of activation of G proteins.

The effect of OA1 intracellular peptides on both the activity and structural stability of G protein was investigated. The intracellular peptides were designed from the crystal structures of same family receptors as a region of interaction between G protein and receptor. $G\alpha_i$ activation, monitored by the change in tryptophan fluorescence, has proved that these peptides cause a conformational change in the G protein. Interaction of 'intracellular loop 3' (ICL3) peptide with α-subunit leads to an increase in the rate of activation of WT $G\alpha_{i1}$ (Fig. 7H) and preferentially affecting the activation rates of the mutant proteins. ICL1 and ICL4[F] peptides do not influence activation of $G\alpha_{i1}$ or its mutants, except for the effect of ICL1 peptide on G203A mutant (Fig. 7I, Table 3). Furthermore, the thermal perturbations of the secondary structure of WT $G\alpha_{i1}$ and its mutants demonstrate that the ICL3 region of the OA1 receptor selectively destabilizes the GDP-bound state whereas the GTP-bound state remains unaffected (Fig. 8A–D). The extent of destabilization of the mutant proteins caused by the peptides depends on the fold increase in the rate of activation (compared to wild-type) caused by the mutation – faster the rate of activation (in comparison with wild-type), greater the effect of the peptide. Among the loop peptides, ICL3 peptide caused most destabilization of the GDP-bound state of α5 helix mutants (Fig. 7C and F). The other two mutants have a negligible effect upon addition of the ICL3 peptide (Fig. 7A,B,D,E).

In a sequence of steps required to achieve an active state conformation, the fast acting mutants (A326S and T329A) are possibly in conformational states that enable searching the metastable step easily. Among the other two mutants, G203A is locked in a conformationally restrained state that does not allow $Mg^{2+}$-binding, resulting in loss of activation. On the other hand, Q204L is not different from WT though ICL3 peptide demonstrates an effect on its activation. The wild-type, as evident from the data earlier, will attain a metastable state upon mild perturbance (unfolding) of its global conformation (Fig. 4A). These results provide additional evidence that the receptor-mediated activation of G protein goes through a selective 'metastabilization' of its GDP released state.
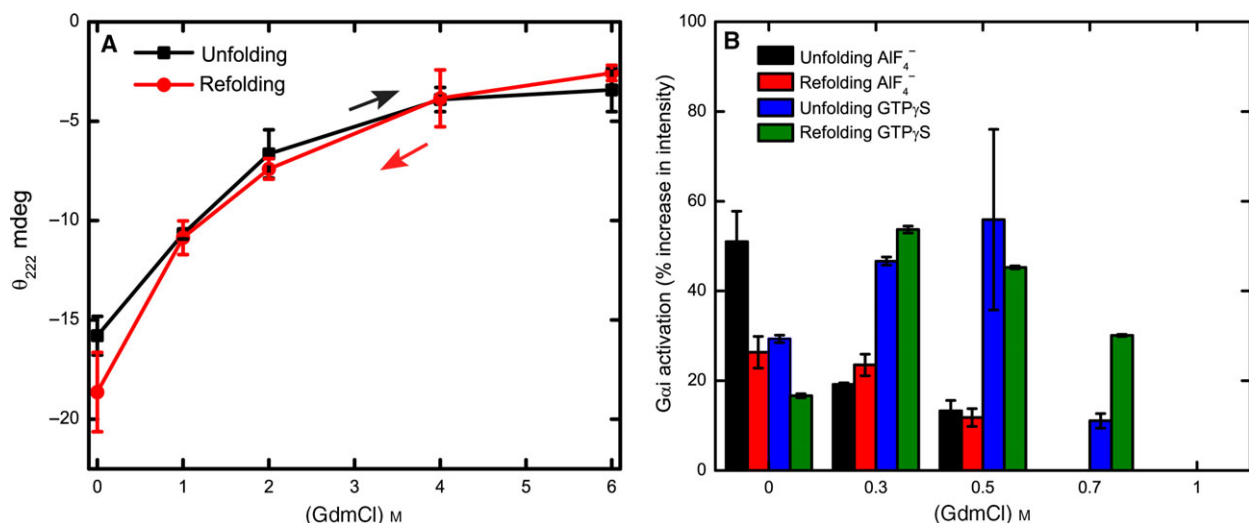
**Fig. 5.** Comparative analysis of the kinetics and activity of refolded Gα$_{i1}$. To ascertain the establishment of chemical equilibrium, the reversibility of unfolding process was monitored using far-UV CD and fluorescence spectroscopy of refolded Gα$_{i1}$ protein. Panel A represents the secondary structural changes monitored by ellipticity variations at 222 nm of the unfolded (black) and refolded (red) GDP-bound Gα$_{i1}$ (5 μM) at various concentrations of GdmCl. The refolded protein exhibited secondary structural characteristics similar to that observed in unfolded protein at the respective GdmCl concentrations. Panel B represents the activation profile of unfolded and refolded GDP-bound Gα$_{i1}$ (0.2 μM) ascertained by monitoring the enhancement of fluorescence intensity at 340 nm on the addition of AlF$_4^-$ and GTPγS at various GdmCl concentrations. Activation of the refolded protein (signifying the uptake and exchange in guanine nucleotides) is observed at similar GdmCl concentrations as that of the unfolded protein. The data shown in panels A and B are representative of an average of three independent experiments and corresponding error plots are calculated from the standard deviations.
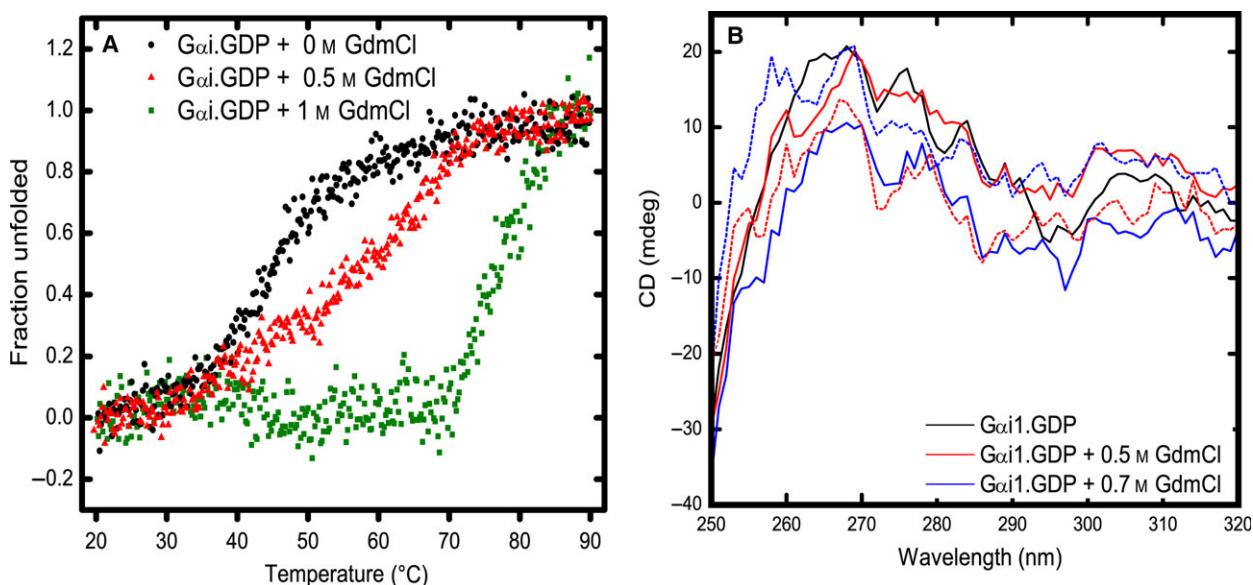


**Fig. 6.** Thermal stability and tertiary structural changes of refolded Gα$_{i1}$. The thermal stability of refolded protein is studied. Panel A depicts the thermal stability of refolded Gα$_{i1}$ protein ascertained by CD measurements in the far UV region reflecting secondary structural transitions. These changes in ellipticity at 222 nm are represented as fraction unfolded of refolded GDP-bound Gα$_{i1}$ (5 μM) at 0 M (black), 0.5 M (red), and 1 M (green) GdmCl concentrations with varying temperature between 20 °C and 90 °C. The thermal stability profile of refolded protein at different GdmCl concentrations (0 M, 0.5 M, and 1 M) is similar to that of the unfolded protein, with a significant $T_m$ shift of enhanced stability at 1 M of GDP-bound configuration. Panel B depicts the tertiary structure of Gα$_{i1}$ studied by near-UV CD spectroscopy of unfolded (bold lines) and refolded protein (dashed lines) at 25 °C. Near-UV CD spectra is collected from 250 to 320 nm with 2 nm slit width at a scanning rate of 50 nm·min$^{-1}$ and an average of three spectra is depicted here.
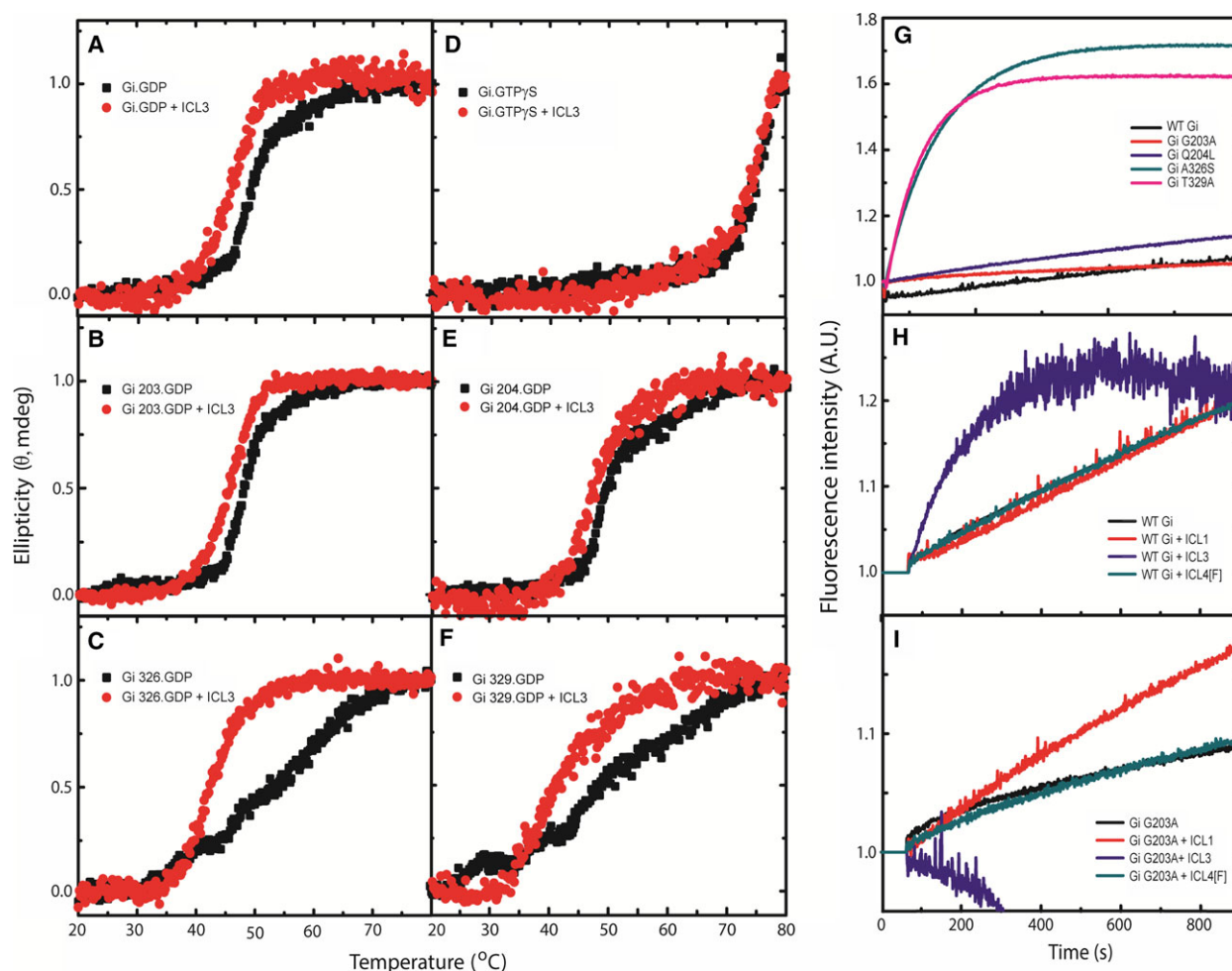
**Fig. 7.** Gα$_{i1}$ mutants representing a variety of signaling states vary in their capacity to form the metastable state. The secondary structure content at 222 nm is plotted as a function of temperature to monitor the global unfolding of Gα$_{i1}$ (5.5 μM). Panel A represents the GDP-bound conformation of Gα$_{i1}$ in the absence (black trace, apparent $T_m$ is 50 °C) and presence of ICL3 peptide (40 μM; red trace, apparent $T_m$ is 45 °C) whereas panel D represents the GTPγS-bound conformation of Gα$_{i1}$ in the absence (black trace, apparent $T_m$ is 77 °C) and presence of ICL3 peptide (40 μM; red trace, apparent $T_m$ is 77 °C). Panels B, E, C, and F represent the GDP-bound states of Gα$_{i1}$ point mutants G203A (inactive, apparent $T_m$ is 47.5 °C), Q204L (active, apparent $T_m$ is 50 °C), A326S (fast acting, apparent $T_m$ is 55 °C), and T329A (fast acting, apparent $T_m$ is 55 °C), respectively, in the absence (black trace) and presence of ICL3 peptide (40 μM; red trace, apparent $T_m$ is 45 °C, 50 °C, 42.5 °C, and 42.5 °C for G203A, Q204L, A326S, and T329A mutants respectively). The right side panels represent fluorescence emission of 200 nM protein at 340 nm. Panel G depicts the basal nucleotide exchange rates of WT Gα$_{i1}$ (black) and its mutants G203A (red), Q204L (blue), A326S (dark cyan), and T329A (pink). Panels H and I represent the activation time course of WT Gα$_{i1}$ and G203A, respectively, in the presence of saturating concentrations of 50 μM ICL1 peptide (red), 45 μM ICL3 peptide (blue), and 35 μM ICL4[F] peptide (dark cyan) and the trace of the respective proteins in the absence of peptides is shown in black color.

# Discussion

G proteins are highly conserved molecular switches, vital to all organisms and are activated by membrane-bound 7 TM GPCRs [31,32]. Fidelity to guanine nucleotide is the hallmark of the 'design principle' of their structural architecture. Catalyzed by the membrane-bound receptor, they undergo the GTPase cycle, GDP release being the rate-limiting step. Even though Gα-subunit proteins from different organisms have

similar sequences and identical structures, they exhibit tremendous variety in rates of nucleotide exchange and hydrolysis [33–36]. Based on the thermodynamic stabilities, the GDP-bound form has been predicted to be more flexible compared to the GTP-bound form [37]. A point mutation (G202D) in Gα subunit leading to lower stability signifies the link between its structural stability and its function, demonstrated in *Caenorhabditis elegans* [14]. While naturally occurring mutations provide direct insight into the mechanistic basis of

**Table 3.** Initial rates of activation of Gαi1 and its point mutants in the presence of peptides. The apparent rate constants ($K_{app}$) reported is the mean of a set of three independent experiments. The fold change was calculated as the ratio of either the rate of WT ± peptide or mutant protein to that of WT or the rate of Mutant ± peptide with respect to that of the mutant protein. (Notations used in the table are as follows: 'a' corresponds to fold change in G203A with respect to WT, 'a*' corresponds to fold change with respect to that of G203A, 'b' corresponds to fold change in Q204L with respect to WT, 'b*' corresponds to fold change with respect to that of Q204L, 'c' corresponds to fold change in A326S with respect to WT, 'c*' corresponds to fold change with respect to that of A326S, 'd' corresponds to fold change in T329A with respect to WT and 'd*' corresponds to fold change with respect to T329A.

| Protein | Peptide | $K_{app}$ ($\times 10^{-3} \cdot s^{-1}$) | Fold Change |
|---|---|---|---|
| WT Gα$_{i1}$ | No peptide | 0.39 | – |
| | ICL1 | 0.5 | 1.28 |
| | ICL3 | 1.36 | 3.48 |
| | ICL4[F] | 0.43 | 1.1 |
| Gα$_{i1}$ G203A mutant | No peptide | 0.22 | 0.56[a] |
| | ICL1 | 0.26 | 1.18[a*] |
| | ICL4[F] | 0.21 | 0.95[a*] |
| Gα$_{i1}$ Q204L mutant | No peptide | 0.5 | 1.28[b] |
| | ICL1 | 0.47 | 0.94[b*] |
| | ICL4[F] | 0.36 | 0.72[b*] |
| Gα$_{i1}$ A326S mutant | No peptide | 5.1 | 13.07[c] |
| | ICL1 | 6 | 1.18[c*] |
| | ICL4[F] | 6.3 | 1.24[c*] |
| Gα$_{i1}$ T329A mutant | No peptide | 5.9 | 15.12[d] |
| | ICL1 | 6.8 | 1.15[d*] |
| | ICL4[F] | 6.1 | 1.03[d*] |

human diseases, several recombinantly engineered mutations have provided a great understanding of the structure–function relationship of the α-subunit [7,27,38,39]. Most recent literature has focused on the importance of the structural integrity of C-terminal α5 helix of the protein [4,11,40,41]. Analysis of the crystal structure accompanied by biochemical experiments revealed important residues involved in activation and prompted the hypothesis that movement of the C-terminal α5 helix (receptor interacting site) and/or opening of the two domains leads to the release of the bound GDP [9,11,29,42].

Understanding of the activation mechanism of G proteins took a paradigm shift with the advent of the crystal structure of the ternary complex (of the receptor and the G protein) [4]. The receptor-bound α-subunit in the complex, with its two domains positioned away from each other, threw open more questions. In fact, the crystal structure of the complex is one among an ensemble of differently stabilized structures, as is evident from electron microscopic studies of the ternary

complex [13]. In the present study, we demonstrate the ability to trap a nucleotide-free ('empty pocket') conformational state of the protein is a key step in the activation process. We provide evidence that the receptor leads the GDP-bound α-subunit to the 'empty pocket state' by mildly perturbing its conformation, holding it in a 'metastable' structure, to achieve activation.

Our conclusions emanate from quantitative determination of the structural stabilities (temperature- and GdmCl-mediated) and complexities of different conformational states of Gα$_{i1}$, arising due to the type of nucleotide bound. Even as the thermal stability of WT Gα$_{i1}$ has been alluded to previously, there is no mechanistic information on the unfolding complexities and hence the stability of G proteins being related to their function [14,22,29,43,44]. The enhanced thermal stability of the 'metastable state' (nucleotide-free state) is highlighted with a stable conformation and its ability to bind GTP. Significant differences in the stabilities of the point mutants (reported in the literature to have differences in activation rates) support the proposed mechanism of activation. Comparative analysis of the stability signatures of these select mutants with WT and the differences caused by a receptor-based peptide (ICL3) signify that the effect of mutations on the stability originate from the altered and novel structural folds of Gα$_{i1}$. Receptor-based peptides are chosen over the full receptor experimental ease. The most prominent effect on the stability observed is in the GTP-bound form of the constitutively inactive G203A mutant. The drop of the apparent $T_m$ to 52.5 °C (for the mutant) as compared to 72 °C of the GTP-bound wild-type signifies a loss of conformational plasticity *en route* stabilization and validates our hypotheses that metastable conformation (highly stable, nucleotide-free form) is essential for activation. $T_m$ of the mutant's GTP-bound structure resembling the wild-type GDP-bound α-subunit further strengthens our proposition that the route to meta-stabilization was significantly lost due to the mutation and therefore exhibits a low $T_m$. Formation of metastable conformation is affirmed with an increase in hydrophobicity around tryptophan residue in GTP-bound conformations of WT and constitutively active mutant (Q204L) during thermal unfolding. Additionally, the stability of the active conformation (GTP-bound form) of mutants in the α5 helix is slightly lower than that of WT, a fact not evident from their crystal structures [27,28]. These observations imply that the predetermined core integral structure of the protein is changed subtly by the receptor and also matches the previously reported 'melting' (and therefore disturbing the overall structural stability of the protein) of the α5 helix as a vital step toward activation [9].
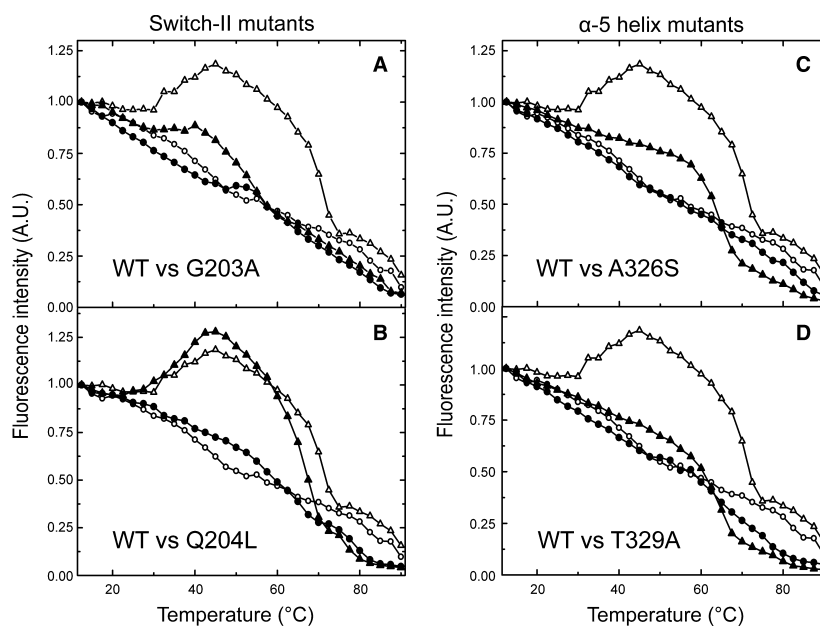
**Fig. 8.** Conformational differences in active state between wild-type and mutants. Tryptophan fluorescence emission maxima are plotted as a function of temperature to monitor the thermal unfolding of WT $G\alpha_{i1}$.GDP (open circle), WT $G\alpha_{i1}$.GTPγS (open triangle) in comparison to that of the mutant $G\alpha_{i1}$.GDP (closed circle) and mutant $G\alpha_{i1}$.GTPγS (closed triangle). Panels A, B, C, and D represent the thermal unfolding plots of the point mutants G203A, Q204L, A326S, and T329A respectively. For all the panels, the emission intensity value corresponding to the lower limit of temperature has been normalized to 1. Each panel is representative of the mutant spectra compared with that of the wild-type. Except for Q204L (Panel B), the thermal unfolding profile of the active state of other mutants differs markedly from that of the wild-type. Both WT and Q204L mutant demonstrate enhanced emission intensities of their active state conformation between 30 °C and 50 °C. All the experiments were performed in buffer containing 10 mM HEPES (pH: 7.5), 2 mM $MgCl_2$, 50 mM NaCl, and 10 μM GDP. Nucleotide exchange in GDP for GTP in $G\alpha_{i1}$ was initiated by incubating the protein with 100 μM GTPγS (50-fold excess) on ice for 1 h.

Changes in transition states during the unfolding process (between the three ligand bound forms) indicate the complex structural fold of $G\alpha_{i1}$ in GDP-bound conformation, as revealed from complex pattern upon chemical perturbation of various ligand forms. A remarkable feature of GdmCl-induced unfolding transitions of $G\alpha_{i1}$ in GDP-bound state is the presence of a stable intermediate secondary structure (between 0.8 and 1.5 M GdmCl), emanating from the partial restructuring of the protein, as evident from fluorescence and thermal studies indicates the metastable conformation. Fall in 8-anilino-1-naphthalene sulfonic acid (ANS) binding between 0.8 and 1 M GdmCl is probably due to a collapse of the hydrophobic residues into the inside the protein structure [45]. This observation also fits well with the model proposed by Hamm and Hubble demonstrating the melting of the α5 helix and/or restructuring the global conformation in the process of activation [14,46].

Loss of bound GDP at 0.7 M GdmCl and metastabilization of the empty pocket structure at 1 M GdmCl are indicative of the structural snapshots of how the receptor might selectively destabilize GDP-bound state to achieve and stabilize 'empty pocket' confirmation of the Gα protein. GdmCl driven 'empty pocket' state is met with success in trapping the unbound conformation while the previous studies tend to achieve this state only in presence of receptor and recombinant Gα protein formed aggregates in absence of GDP. To test whether receptors mediate activation of G protein by partial/selective destabilization of its GDP-bound structure, we monitored the effect of intracellular peptides of OA1 receptor on the stabilities of $G\alpha_{i1}$ and its mutants in their inactive and active state conformations. Mutational analyses of the receptor cytoplasmic loop regions (in literature) have clearly demonstrated these regions to be involved in G protein recognition, selectivity, coupling, and activation. Receptor peptides do affect the activation properties of the cognate G protein [19,47]. It is from this perspective that receptor peptides pertaining to the cytoplasmic domain regions have been tested for their interaction with the G protein. However, the soluble receptor peptides alone may/will not exhibit the potential activation mediated by the whole receptor. Thereby, we do not expect the receptor peptides alone to cause rotation and translation of the α5 helix. What

we expect and speculate is that the charged perturbations caused by receptor peptides might weaken the core integrity of the nucleotide domain. Moreover, the addition of these peptides does alter the activity of the G alpha protein as described in our results. The extent of destabilization matches the relative ease of activation of the mutants (T329A > A326S > Q204L > G203A) being locked in a partially perturbed GDP-bound conformation (T329A and A326S), else being locked in a conformation not accessible to activation (represented by G203A) and thereby having lost the ability to adopt the metastable structure. This is also supported by the physiological observation that the G202D mutation causes instability in the protein and leads to faster activation rates [14]. Furthermore, refolding studies (structural and activation) corroborate the existence of thermodynamic equilibrium and also establish the ability to retake guanine nucleotide to an unliganded empty state Gα protein. However, in the case of thermal stress, such reversibility was abrogated with the formation of an aggregated intermediate with residual β-sheet structure, succeeding the loss of guanine nucleotide. Similar attempts at refolding the Gα from inclusion bodies (solubilized in 8 M urea) has met with limited success, wherein the ability to rebind nucleotides and regain native structure was only partially possible [15]. Reconciliation of these observations perpetuates the view that the ephemeral intermediate empty pocket state structure requires stabilization of the exposed hydrophobic regions (shown by ANS binding) by a noncovalent hydrophobic scaffold of the receptor or due to shielding of the solvation effect by GdmCl. In lieu of the absence of such interactions, exposed hydrophobic clusters aggregate to shield themselves from aqueous solution necessitating the supplementation of nucleotide protection to prevent such irreversible aggregation [23].

Previous work (MD simulations [48] supported by experimental data) states that the receptor complex like the structure of G protein can be trapped only in the absence of guanine nucleotides [4]. Domain separation has been demonstrated in the literature of the protein alone or upon interaction with Ric-8 [18]. Our results here, demonstrating the rapid uptake of GTP by protein and the concurrent inability to bind $AlF_4^-$, both in the proteins' unfolding and the refolding pathway clearly indicate the presence of a very stable empty pocket state. Our studies support the view that domain separation follows nucleotide release (loss of GDP) caused by the receptor. Reversibility of the protein fold (upon removal of a chaotrope) of G protein alpha subunit also reinforce the view that structural perturbations are not only quintessential for GDP release and meta-stabilization of empty pocket structure but also the dynamics of such changes are dependent on the exit of GDP from the protein.

These results demonstrate that GPCRs catalyze the nucleotide exchange by selective destabilization of the GDP-bound state by partial unfolding of the structural segments, causing the release of the bound nucleotide and maintaining a 'metastable' empty pocket structure, as may be seen in the latest crystal complex of beta-adrenergic receptor 2 (β 2AR) and Gα$_s$ [4]. Using equilibrium unfolding experiments with Gα protein, we elucidate the basis of structural switching and demonstrate evidence for the existence of a metastable, GDP released, state that offers a clue to the mechanism of activation. The metastable intermediate structure offers insight into the probable switched structural conformation in order to be able to bind GTP (Fig. 9). A recent finding that suggests a conformational transition of GDP to GTP exchange in the monomeric GTPase 'Arf6' ensues by partial unfolding of its GDP-bound state and provides support to our observations [49]. Therefore, we propose that GPCRs catalyze the nucleotide exchange by selective perturbance of the GDP-bound conformation of G protein to a metastable intermediate structural state (mimicked by 0.5/0.7 M GdmCl in Gα$_{i1}$) and accelerate the rate-limiting step of GDP release by surpassing the kinetic barrier (0.2 M GdmCl in Gα$_{i1}$; Fig. 9). This work provides new avenues to study the solution-state structure of the empty pocket state. It is also imperative and important to realize that this type of (spectroscopic) study cannot be performed on the heterotrimeric protein. Experiments are in progress in our lab to achieve similar goals/results using other techniques.

# Materials and methods

## Chemicals and reagents

GDP sodium salt and GTPγS tetra lithium salt were purchased from Sigma-Aldrich (Germany). Point mutants of WT Gα$_{i1}$ were generated by site-directed mutagenesis using the Quick Change XL-II mutagenesis kit (Stratagene, La Jolla, CA, USA ). The chaotrope, GdmCl (8 M solution) was purchased from Thermo Fischer (Waltham, MA, USA). All other reagents and chemicals used were purchased locally and were of the highest purity.

## Synthetic peptides

Synthetic peptides derived from the predicted cytoplasmic loop regions of the human OA1 receptor were purchased commercially. Sequences of the peptides and their names (used in this study) are mentioned in Table 4. Peptide
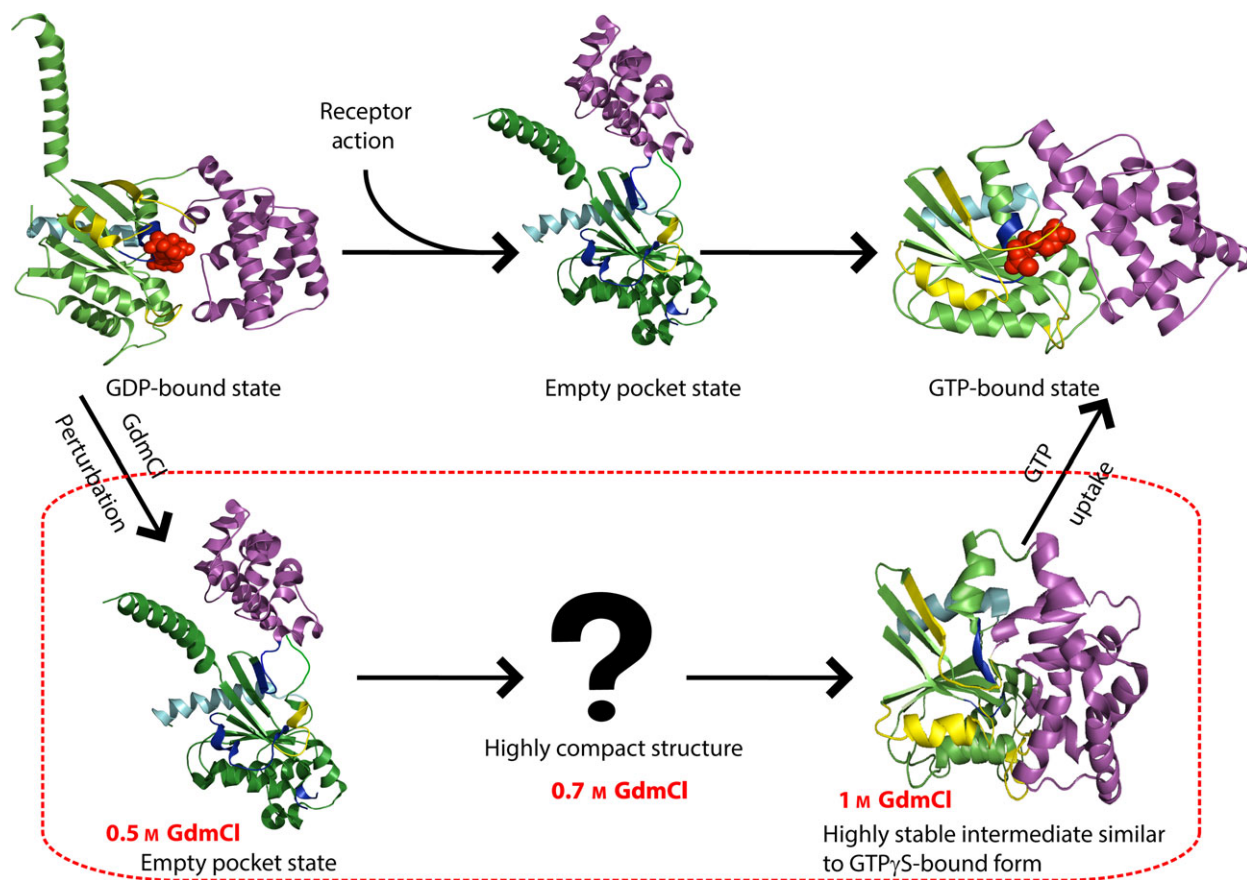
**Fig. 9.** Model for activation mechanism of G proteins. The model emerging from the results presented here is that the empty pocket state of the G protein α-subunit adopts a compact conformation that is as stable as the activated (GTP-bound) state of the protein during the process of activation (upper three indicative structures). The same 'metastable' state can be replicated by partially perturbing the protein structure by submolar concentration of GdmCl. While at 0.7 M GdmCl a highly compact structure is observed, further perturbation leads to a meta-stable state at 1 M GdmCl (lower three indicative structures). The function of the receptor in the process of activating the G protein is to enable a subtle change in α-subunit conformation so that the bound nucleotide is released and the protein achieves a metastable conformation.

**Table 4.** Synthetic peptides corresponding to the ICL regions of the human OA1 receptor. The numbers denoted with pointed arrows in the sequence represent the amino acid positions in the primary sequence of the full-length receptor. The underlined and italicized amino acids represent the probable transmembrane regions. 'W' at position 313 of the native intracellular loop 4 sequence designated as ICL4[W] was replaced with 'F', denoted as ICL4[F] and shown in italicized bold.

| Peptide | Length in amino acids | Sequence |
| --- | --- | --- |
| ICL1 | 30 | [50]FPGRRPAGPGSPATSPPASVRILRAAAACD[78] |
| ICL3 | 36 | [213]F*QKTVTAVASLLK*GROGIYTENERRMGAVIKIRFFK[248] |
| ICL4[F] | 27 | [309]*AFYGF*TGCSLGFQSPRKEIQFESLTTS[335] |
| ICL4[W] | 27 | [309]*AFYGW*TGCSLGFQSPRKEIQFESLTTS[335] |

representing intracellular region 4 (ICL4) loops include a helical segment of the cytoplasmic ends of TM6 and TM7. Lyophilized peptides were dissolved in molecular biology grade water except for ICL4[W] peptides, which were solubilized in 50% acetonitrile. All titration experiments were

performed in aqueous buffer without any organic solvent. Scrambled peptides were not used for controls as extensive data are available that demonstrates mutations in many receptors (single amino acid or deletions of regions) affecting activation of G proteins [47,50–52].

## Subcloning of Gαi1 into pTYB12

Recombinant rat Gα$_{i1}$, previously expressed using pET28a expression vector, was subcloned into pTYB12 vector (New England Biolabs, Ipswich, MA, USA) using the restriction sites *Nhe*I and *Xho*I. The double digested vector was ligated with the double digested Gα$_{i1}$ insert (~ 1 kb) from pET28a vector and 700 bp smaller released fragment of the vector backbone. Recombinant clones were screened for the presence of a double insert by colony PCR using intein forward and T7 terminator primers respectively. The positive clone was further verified by restriction digestion and confirmed by PCR-based nucleotide sequencing. Protein was expressed as a fusion to the C-terminus of chitin bound-intein tag, which is self-cleavable upon incubation with dithiothreitol (DTT), releasing an 'untagged' protein.

## Construction of Gαi1 mutants

Site-specific point mutations in Gα$_{i1}$ were introduced with Quick Change system (Stratagene). Four proteins with G203A, Q204L, A326S, and T329A point mutations were selected for the study. Mutagenesis reaction was done in 50 µL total volume using 40 ng of template DNA and all other reagents were added following the Quick Change XL-II site-directed mutagenesis kit instructions (Stratagene). About 2 µL of the digested DNA was used for transformation of Gold competent cells into *Escherichia coli* XL-10 and plated for selection of ampicillin-resistant clones. Mutations were confirmed by sequencing the plasmid DNA.

## Overexpression and purification of Gαi1

Recombinant rat Gα$_{i1}$ and its mutants were expressed in *E. coli* BL21 (DE3) cells grown in the presence of ampicillin (100 µg·mL$^{-1}$). Typically, 1 L of cell culture was grown at 37 °C till the value of A$_{600}$ nm reached 0.5 and then induced with 200 µM isopropyl-β-D-thiogalactoside (IPTG). The culture was then grown for 16–24 h at 23 °C at an agitation speed of 180 r.p.m. Cells were harvested by centrifugation at 18 500 *g* for 5 min at 4 °C and the pellet was stored at −80 °C.

All protein purification procedural steps were carried out at 4 °C. For lysis, the stored cell pellets were thawed on ice and resuspended in a buffer containing 20 mM TRIS (pH 8.0), 100 mM NaCl, 2 mM MgCl$_2$, and 10 µM GDP (resuspension buffer), and sonicated using an ultrasonicator (Vibracell Sonics and Materials, Inc. Newtown, CT, USA). The cell lysate was then centrifuged at 4 °C (18 500 *g* for 45 min) and the resulting supernatant fraction was loaded onto a chitin resin (New England Biolabs) containing column previously equilibrated with 20 mM TRIS (pH 8.0), 100 mM NaCl, 2 mM MgCl$_2$, and 10 µM GDP (equilibration buffer). The protein-loaded resin was washed with 40 column volumes (C.V.) of Wash buffer (equilibration buffer

with 300 mM NaCl) and then flushed with 3 C.V. of cleavage buffer (equilibration buffer with 50 mM DTT). Gα$_{i1}$ and mutants were released from the chimera by incubation at 4 °C for 20 h to trigger the self-cleavage of the intein tag. Flow through from the column was collected, pooled and concentrated to a volume of 1 mL using a 10 kDa cut-off membrane concentrator (Millipore Corp., Bedford, MA, USA). Purified protein was used within a period of 2 weeks. This bacterially expressed protein has been reported to mimic *in vivo* situation accurately in several instances, including the ternary crystal complex [53].

## Fluorescence spectroscopy

Fluorescence measurements were carried out on a fluorolog-3 fluorimeter (Horiba Jobin Yvon, Edison, NJ, USA) equipped with a 450 W Xenon arc lamp. Fluorescence titration experiments were performed in 20 mM TRIS buffer (pH 7.5) containing 100 mM NaCl, 2 mM MgCl$_2$, 1 mM DTT, and 10 µM GDP. Protein fluorescence was recorded by exciting the sample at 295 nm and emission monitored from 310 to 400 nm. The excitation and emission slit band pass were set at 5 and 15 nm respectively. Titration experiments were typically performed by adding 3.75 µL aliquots of the peptide from a stock solution of 1 mM to a 750 µL protein solution of 200 nM. Thermal unfolding studies were performed by varying the sample temperature from 10 to 90 °C with an interval of 2.5 °C on a Perkin Elmer LS55 fluorimeter equipped with a thermostat ($\lambda_{ex}$ = 295 nm and $\lambda_{em}$ = 340 nm). G protein activation assay was performed on a Jasco FP-6500 spectrofluorimeter at 25 °C with constant stirring. Gα$_{i1}$ (0.2 µM), in the presence of saturating concentrations of peptides, was incubated in the reaction buffer [20 mM TRIS (pH7.5), 2 mM MgCl$_2$, 1 mM DTT, 1 µM GDP, and 100 mM NaCl] for 5 min. The relative increase in intrinsic fluorescence ($\lambda_{ex}$ = 295 nm, $\lambda_{em}$ = 340 nm) was measured as a function of time by the addition of 100-fold molar excess of GTPγS (50 µM) after a baseline recording of 60 s to initiate the nucleotide exchange. The same procedure was followed up for all Gα$_{i1}$ mutants. It should be noted that addition of GTPγS does not lead to any scattering or background fluorescence, as is also evident from activation assay data. GdmCl induced equilibrium unfolding was carried out by incubating the protein (55 µg·mL$^{-1}$) with increasing concentrations of GdmCl. Protein solutions containing GdmCl were incubated overnight and the fluorescence emission spectrum was measured from 300 to 400 nm by exciting at 295 nm on a Hitachi F-4500 spectrofluorimeter. The spectra were recorded using an excitation and emission bandpass of 5 nm each at room temperature. A total of 61 points of intrinsic fluorescence data were recorded between 0 and 6 M GdmCl with increments of 0.1 M each for Gα$_{i1}$ in the presence of GDP and GTPγS. Fluorescence intensity of native protein (without GdmCl) was taken as 100% native, and

the fraction of unfolded molecules was calculated accordingly. Thermodynamic parameters are measured using standard multistate unfolding equation available in the literature using GRAPHPAD Prism 5.0 (La Jolla, CA, USA). Each fractional transition step is calculated and fit from residuals of the unfolding equation [54]. For ANS binding experiments, 1 μM Gα$_{i1}$ protein solution in GDP-bound state was incubated with 10 μM of ANS (stock prepared in methanol and diluted to the required concentration in the buffer) for ~ 30 min. The mixture was then excited at 360 nm and the fluorescence emission was recorded between 400 and 600 nm on Jasco FP-6500 spectrofluorimeter at 25 °C. The excitation and emission slit band pass were set at 5 and 15 nm respectively. ANS spectra were corrected for ANS fluorescence taken in the buffer. Affinity and stoichiometry of the interactions were calculated by nonlinear regression analysis of one-site saturation binding using the software GRAPHPAD Prism 5.0 by the following equation:

$$Y = B_{max} \times X / (K_d \times X)$$

### Circular dichroism (CD) spectroscopy

The stability of WT Gα$_{i1}$ and its mutants in GDP- and GTPγS-bound forms was investigated by monitoring changes induced at a fixed wavelength (222 nm; negative CD band typical of alpha-helix conformation) while varying the temperature from 20 to 80 °C by every 1 °C on a Jasco-815 spectropolarimeter equipped with a thermostat. Near-UV CD spectra of 30 μM protein was recorded from 250 to 320 nm at a rate of 50 nm·min$^{-1}$ with 2 nm slit width at 25 °C and corresponding buffer signal is subtracted from the sample. All CD experiments were performed in reaction buffer as mentioned earlier.

### Differential scanning calorimetry (DSC)

Differential scanning calorimetry scans from 10 to 90 °C at the rate of 60 °C·h$^{-1}$ were recorded on a VP-DSC microcalorimeter (Microcal Inc., Westborough, MA, USA). The appropriate buffer was used to establish the baseline before introducing the protein solution prepared in the same buffer and the data were analyzed using the MICROCAL Origin 7.0 software supplied by the vendor. The effect of peptides on the thermal unfolding of the protein was also monitored. All thermal studies (CD melting and DSC) were performed in HEPES buffer.

### Refolding of Gαi1

Refolding profile of Gα$_{i1}$ was studied using far-UV CD, fluorescence spectroscopy, and thermal stability assays. The total unfolding of Gα$_{i1}$ was carried out by incubating the protein in 8 M GdmCl for 1 h at room temperature. Refolding was initiated by diluting the sample to appropriate GdmCl concentration with refolding buffer (20 mM HEPES pH 7.4, 100 mM NaCl, 2 mM MgCl$_2$, 1 μM GDP with corresponding GdmCl concentrations) and incubated for 4 h at room temperature. Far-UV CD measurements were performed with 5 μM protein concentration in Jasco CD spectropolarimeter. The observed ellipticity (θ$_{222}$) values are plotted as a function of GdmCl concentration to obtain the secondary structural changes and depict the unfolding and refolding profile of the protein. Functional activity for unfolded and refolded Gα$_{i1}$ (recorded using changes in tryptophan fluorescence), was analyzed by AlF$_4^-$ binding and GTPγS uptake [55]. Fluorescence spectra were recorded by exciting the samples (0.2 μM of Gα$_{i1}$) at 295 nm and monitoring emission intensity from 310 to 440 nm keeping excitation and emission bandpass of 5 nm. The presence of bound GDP in Gα$_{i1}$ was assessed by addition of AlF$_4^-$ (formed by adding 10 mM NaF and 30 μM AlCl$_3$) and fluorescence spectra were immediately recorded. Likewise, the activation kinetics of refolded Gα$_{i1}$ was studied by triggering basal nucleotide exchange property of Gα$_{i1}$ on the addition of 50 μM GTPγS, and the corresponding fluorescence spectra recorded after an incubation of 5 min at room temperature. Percentage increase in fluorescence intensity upon activation and exchange is calculated as follows,

$$\% \text{ Increase in fluorescence intensity} = (I_{AlF/GTP\gamma S} - I_{GDP}) \times 100 / (I_{GDP})$$

where $I_{GDP}$ denotes fluorescence intensity at 340 nm in GDP-bound form (inactive state) and $I_{AlF/GTP\gamma S}$ denotes fluorescence intensity at 340 nm in AlF$_4^-$ or GTPγS bound conformation. This % increase in fluorescence intensity is used to analyze the behavior of unfolded and refolded protein in the above-mentioned activation methods.

Thermal stability of refolded Gα$_{i1}$ was monitored by recording the secondary structural changes using ellipticity values at 222 nm using far-UV CD spectroscopy with a gradual increase in temperature from 20 to 80 °C controlled by a thermostat.

## Acknowledgments

## Author contributions

SKA and GKA conceived and coordinated the study and wrote the paper. SKA designed, performed and

analyzed experiments shown in Figs 1–4 and 7–9. RV performed experiments shown in Figs 5–6. SKA and RV prepared the figures. All authors reviewed the results and approved the final version of the manuscript.

## Conflict of interest

The authors declare that they have no conflicts of interest with the contents of this article.

## References

1 Offermanns S (2003) G-proteins as transducers in transmembrane signalling. *Prog Biophys Mol Biol* **83**, 101–130.

2 Sprang SR (1997) G protein mechanisms: insights from structural analysis. *Annu Rev Biochem* **66**, 639–678.

3 Tesmer JJ (2010) The quest to understand heterotrimeric G protein signaling. *Nat Struct Mol Biol* **17**, 650–652.

4 Rasmussen SG, DeVree BT, Zou Y, Kruse AC, Chung KY, Kobilka TS, Thian FS, Chae PS, Pardon E, Calinski D *et al.* (2011) Crystal structure of the beta2 adrenergic receptor-Gs protein complex. *Nature* **477**, 549–555.

5 Aris L, Gilchrist A, Rens-Domiano S, Meyer C, Schatz PJ, Dratz EA & Hamm HE (2001) Structural requirements for the stabilization of metarhodopsin II by the C terminus of the alpha subunit of transducin. *J Biol Chem* **276**, 2333–2339.

6 Cherfils J & Chabre M (2003) Activation of G-protein Galpha subunits by receptors through Galpha-Gbeta and Galpha-Ggamma interactions. *Trends Biochem Sci* **28**, 13–17.

7 Marin EP, Krishna AG & Sakmar TP (2001) Rapid activation of transducin by mutations distant from the nucleotide-binding site: evidence for a mechanistic model of receptor-catalyzed nucleotide exchange by G proteins. *J Biol Chem* **276**, 27400–27405.

8 Noel JP, Hamm HE & Sigler PB (1993) The 2.2 A crystal structure of transducin-alpha complexed with GTP gamma S. *Nature* **366**, 654–663.

9 Oldham WM, Van Eps N, Preininger AM, Hubbell WL & Hamm HE (2006) Mechanism of the receptor-catalyzed activation of heterotrimeric G proteins. *Nat Struct Mol Biol* **13**, 772–777.

10 Rondard P, Iiri T, Srinivasan S, Meng E, Fujita T & Bourne HR (2001) Mutant G protein alpha subunit activated by Gbeta gamma: a model for receptor activation? *Proc Natl Acad Sci USA* **98**, 6150–6155.

11 Van Eps N, Preininger AM, Alexander N, Kaya AI, Meier S, Meiler J, Hamm HE & Hubbell WL (2011) Interaction of a G protein with an activated receptor opens the interdomain interface in the alpha subunit. *Proc Natl Acad Sci USA* **108**, 9420–9424.

12 Abdulaev NG, Ngo T, Ramon E, Brabazon DM, Marino JP & Ridge KD (2006) The receptor-bound "empty pocket" state of the heterotrimeric G-protein alpha-subunit is conformationally dynamic. *Biochemistry* **45**, 12986–12997.

13 Westfield GH, Rasmussen SG, Su M, Dutta S, DeVree BT, Chung KY, Calinski D, Velez-Ruiz G, Oleskie AN, Pardon E *et al.* (2011) Structural flexibility of the G alpha s alpha-helical domain in the beta2-adrenoceptor Gs complex. *Proc Natl Acad Sci USA* **108**, 16086–16091.

14 Johnston CA, Afshar K, Snyder JT, Tall GG, Gonczy P, Siderovski DP & Willard FS (2008) Structural determinants underlying the temperature-sensitive nature of a Galpha mutant in asymmetric cell division of *Caenorhabditis elegans*. *J Biol Chem* **283**, 21550–21558.

15 McCusker E & Robinson AS (2008) Refolding of G protein alpha subunits from inclusion bodies expressed in *Escherichia coli*. *Protein Expr Purif* **58**, 342–355.

16 Zhang J & Matthews CR (1998) Ligand binding is the principal determinant of stability for the p21(H)-ras protein. *Biochemistry* **37**, 14881–14890.

17 Schiaffino MV & Tacchetti C (2005) The ocular albinism type 1 (OA1) protein and the evidence for an intracellular signal transduction system involved in melanosome biogenesis. *Pigment Cell Res* **18**, 227–233.

18 Tall GG, Krumins AM & Gilman AG (2003) Mammalian Ric-8A (synembryn) is a heterotrimeric Galpha protein guanine nucleotide exchange factor. *J Biol Chem* **278**, 8356–8362.

19 Fahmy K & Sakmar TP (1993) Regulation of the rhodopsin-transducin interaction by a highly conserved carboxylic acid group. *Biochemistry* **32**, 7229–7236.

20 Faurobert E, Otto-Bruc A, Chardin P & Chabre M (1993) Tryptophan W207 in transducin T alpha is the fluorescence sensor of the G protein activation switch and is involved in the effector binding. *EMBO J* **12**, 4191–4198.

21 Hamm HE, Meier SM, Liao G & Preininger AM (2009) Trp fluorescence reveals an activation-dependent cation-pi interaction in the Switch II region of Galphai proteins. *Protein Sci* **18**, 2326–2335.

22 Thomas CJ, Briknarova K, Hilmer JK, Movahed N, Bothner B, Sumida JP, Tall GG & Sprang SR (2011) The nucleotide exchange factor Ric-8A is a chaperone for the conformationally dynamic nucleotide-free state of Galphai1. *PLoS ONE* **6**, e23197.

23 Zelent B, Veklich Y, Murray J, Parkes JH, Gibson S & Liebman PA (2001) Rapid irreversible G protein alpha subunit misfolding due to intramolecular kinetic bottleneck that precedes Mg2+ "lock" after GTP/GDP exchange. *Biochemistry* **40**, 9647–9656.

24 Kumar R, Prabhu NP, Yadaiah M & Bhuyan AK (2004) Protein stiffening and entropic stabilization in the subdenaturing limit of guanidine hydrochloride. *Biophys J* **87**, 2656–2662.

25 Zarrine-Afsar A, Mittermaier A, Kay LE & Davidson AR (2006) Protein stabilization by specific binding of guanidinium to a functional arginine-binding surface on an SH3 domain. *Protein Sci* **15**, 162–170.

26 Naika GS & Tiku PK (2010) Characterization of functional intermediates of endoglucanase from Aspergillus aculeatus during urea and guanidine hydrochloride unfolding. *Carbohydr Res* **345**, 1627–1631.

27 Kapoor N, Menon ST, Chauhan R, Sachdev P & Sakmar TP (2009) Structural evidence for a sequential release mechanism for activation of heterotrimeric G proteins. *J Mol Biol* **393**, 882–897.

28 Posner BA, Mixon MB, Wall MA, Sprang SR & Gilman AG (1998) The A326S mutant of Gialpha1 as an approximation of the receptor-bound state. *J Biol Chem* **273**, 21752–21758.

29 Coleman DE, Berghuis AM, Lee E, Linder ME, Gilman AG & Sprang SR (1994) Structures of active conformations of Gi alpha 1 and the mechanism of GTP hydrolysis. *Science* **265**, 1405–1412.

30 Berghuis AM, Lee E, Raw AS, Gilman AG & Sprang SR (1996) Structure of the GDP-Pi complex of Gly203->Ala gialpha1: a mimic of the ternary product complex of galpha-catalyzed GTP hydrolysis. *Structure* **4**, 1277–1290.

31 Birnbaumer L (2007) The discovery of signal transduction by G proteins: a personal account and an overview of the initial findings and contributions that led to our present understanding. *Biochim Biophys Acta* **1768**, 756–771.

32 Simon MI, Strathmann MP & Gautam N (1991) Diversity of G proteins in signal transduction. *Science* **252**, 802–808.

33 Jones JC, Jones AM, Temple BR & Dohlman HG (2012) Differences in intradomain and interdomain motion confer distinct activation properties to structurally similar Galpha proteins. *Proc Natl Acad Sci USA* **109**, 7275–7279.

34 Lambright DG, Sondek J, Bohm A, Skiba NP, Hamm HE & Sigler PB (1996) The 2.0 A crystal structure of a heterotrimeric G protein. *Nature* **379**, 311–319.

35 Nishimura A, Kitano K, Takasaki J, Taniguchi M, Mizuno N, Tago K, Hakoshima T & Itoh H (2010) Structural basis for the specific inhibition of heterotrimeric Gq protein by a small molecule. *Proc Natl Acad Sci USA* **107**, 13666–13671.

36 Wall MA, Coleman DE, Lee E, Iniguez-Lluhi JA, Posner BA, Gilman AG & Sprang SR (1995) The structure of the G protein heterotrimer Gi alpha 1 beta 1 gamma 2. *Cell* **83**, 1047–1058.

37 Sayar K, Ugur O, Liu T, Hilser VJ & Onaran O (2008) Exploring allosteric coupling in the alpha-subunit of heterotrimeric G proteins using evolutionary and ensemble-based approaches. *BMC Struct Biol* **8**, 23.

38 Bosch DE, Willard FS, Ramanujam R, Kimple AJ, Willard MD, Naqvi NI & Siderovski DP (2012) A P-loop mutation in Galpha subunits prevents transition to the active state: implications for G-protein signaling in fungal pathogenesis. *PLoS Pathog* **8**, e1002553.

39 Marin EP, Krishna AG, Archambault V, Simuni E, Fu WY & Sakmar TP (2001) The function of interdomain interactions in controlling nucleotide exchange rates in transducin. *J Biol Chem* **276**, 23873–23880.

40 Chung KY, Rasmussen SG, Liu T, Li S, DeVree BT, Chae PS, Calinski D, Kobilka BK, Woods VL Jr & Sunahara RK (2011) Conformational changes in the G protein Gs induced by the beta2 adrenergic receptor. *Nature* **477**, 611–615.

41 Orban T, Jastrzebska B, Gupta S, Wang B, Miyagi M, Chance MR & Palczewski K (2012) Conformational dynamics of activation for the pentameric complex of dimeric G protein-coupled receptor and heterotrimeric G protein. *Structure* **20**, 826–840.

42 Marin EP, Krishna AG & Sakmar TP (2002) Disruption of the alpha5 helix of transducin impairs rhodopsin-catalyzed nucleotide exchange. *Biochemistry* **41**, 6988–6994.

43 Lambright DG, Noel JP, Hamm HE & Sigler PB (1994) Structural determinants for activation of the alpha-subunit of a heterotrimeric G protein. *Nature* **369**, 621–628.

44 Streiff J, Warner DO, Klimtchuk E, Perkins WJ, Jones K & Jones KA (2004) The effects of hexanol on Galpha(i) subunits of heterotrimeric G proteins. *Anesth Analg* **98**, 660–667, table of contents.

45 Sadqi M, Lapidus LJ & Munoz V (2003) How fast is protein hydrophobic collapse? *Proc Natl Acad Sci USA* **100**, 12117–12122.

46 Preininger AM, Meiler J & Hamm HE (2013) Conformational flexibility and structural dynamics in GPCR-mediated G protein activation: a perspective. *J Mol Biol* **425**, 2288–2298.

47 Auger GA, Pease JE, Shen X, Xanthou G & Barker MD (2002) Alanine scanning mutagenesis of CCR3 reveals that the three intracellular loops are essential for functional receptor expression. *Eur J Immunol* **32**, 1052–1058.

48 Dror RO, Mildorf TJ, Hilger D, Manglik A, Borhani DW, Arlow DH, Philippsen A, Villanueva N, Yang Z, Lerch MT et al. (2015) Signal transduction. Structural basis for nucleotide exchange in heterotrimeric G proteins. *Science* **348**, 1361–1365.

49 Biou V, Aizel K, Roblin P, Thureau A, Jacquet E, Hansson S, Guibert B, Guittet E, van Heijenoort C, Zeghouf M et al. (2010) SAXS and X-ray

crystallography suggest an unfolding model for the GDP/GTP conformational switch of the small GTPase Arf6. *J Mol Biol* **402**, 696–707.

50 Huang Z, Chen Y, Pratt S, Chen TH, Bambino T, Nissenson RA & Shoback DM (1996) The N-terminal region of the third intracellular loop of the parathyroid hormone (PTH)/PTH-related peptide receptor is critical for coupling to cAMP and inositol phosphate/Ca2+ signal transduction pathways. *J Biol Chem* **271**, 33382–33389.

51 Moro O, Lameh J, Hogger P & Sadee W (1993) Hydrophobic amino acid in the i2 loop plays a key role in receptor-G protein coupling. *J Biol Chem* **268**, 22273–22276.

52 Vogel R, Mahalingam M, Ludeke S, Huber T, Siebert F & Sakmar TP (2008) Functional role of the "ionic lock"–an interhelical hydrogen-bond network in family A heptahelical receptors. *J Mol Biol* **380**, 648–655.

53 Greentree WK & Linder ME (2004) Purification of recombinant G protein alpha subunits from *Escherichia coli*. *Methods Mol Biol* **237**, 3–20.

54 Hung HC, Chen YH, Liu GY, Lee HJ & Chang GG (2003) Equilibrium protein folding-unfolding process involving multiple intermediates. *Bull Math Biol* **65**, 553–570.

55 Kleuss C, Raw AS, Lee E, Sprang SR & Gilman AG (1994) Mechanism of GTP hydrolysis by G-protein alpha subunits. *Proc Natl Acad Sci USA* **91**, 9828–9831.